

Fast Online Reinforcement Learning Control using State-Space Dimensionality Reduction

Tomonori Sadamoto¹, *Member, IEEE*, Aranya Chakraborty², *Senior Member, IEEE*, and Jun-ichi Imura³, *Senior Member, IEEE*

Abstract—In this paper, we propose a fast reinforcement learning (RL) control algorithm that enables online control of large-scale networked dynamic systems. RL is an effective way of designing model-free linear quadratic regulator (LQR) controllers for linear time-invariant (LTI) networks with unknown state-space models. However, when the network size is large, conventional RL can result in unacceptably long learning times. The proposed approach is to construct a compressed state vector by projecting the measured state through a projective matrix. This matrix is constructed from online measurements of the states in a way that it captures the dominant controllable subspace of the open-loop network model. Next, a RL-controller is learned using the reduced-dimensional state instead of the original state such that the resultant cost is close to the optimal LQR cost. Numerical benefits as well as the cyber-physical implementation benefits of the approach are verified using illustrative examples including an example of wide-area control of the IEEE 68-bus benchmark power system.

Index Terms—Large-scale Networks, Reinforcement Learning, Dimensionality Reduction

I. INTRODUCTION

Learning theory has been pursued in the domain of control systems since the early 1970's, mostly through system identification and adaptive control [1]-[2]. Starting from the 90's control theorists started taking an active interest in relating learning with optimal control [3]. In particular, reinforcement learning (RL), which was originally developed in the artificial intelligence community, was related to optimal control as they both seek to find policies that minimize cost functions for a given set of tasks [4]. In recent years, RL has been refurbished with renewed enthusiasm in the context of linear quadratic regulator (LQR) designs through several papers such as [5]-[6], and surveys such as [7], [8].

The fundamental idea behind RL-based LQR is to iteratively learn the optimal state-feedback control gain matrix directly from online measurements of the states and inputs without knowing the system model. Among existing RL techniques such as value iteration [9]-[10], a technique known as *policy iteration* has fast convergence [4] when a given policy structure matches the optimal solution. In policy iteration, the system is

initially excited with exploratory noise, followed by gathering sufficient number of state and input samples for updating the parameters of the policy. For LQR this parameter update is performed by least squares. This estimate is thereafter iterated upon till the estimate converges to produce the optimal control gain, amounting to solving the algebraic Riccati equation using state and input data. However, even for a reasonably fast method such as policy iteration, curse of dimensionality continues to be an ongoing debate. One main reason behind this is that the least squares step requires at least $n(n+1)/2$ number of data samples for a unique solution where n is the order of the system. As a result, the computational cost of policy iteration for every iterate is $\mathcal{O}(n^6)$. This can pose a serious challenge for real-time decision-making and control in networks with large values of n .

A few approaches have been proposed to overcome this curse. For example, in [11], [12] the authors have proposed a method to learn decentralized RL-controllers by regarding the interference between various subsystems in a network as an uncertainty. This method, however, is mostly applicable for weakly-connected networks. In the artificial intelligence community, on the other hand, a notion called *state aggregation* has been proposed to overcome the computational bottleneck of RL in controlling Markov decision processes (MDP). The idea here is that instead of the original state-space the decision-maker finds decision vectors in an abstract state-space much faster by treating groups of states as a unit, ignoring irrelevant state information. A number of abstractions have been proposed, for example see [13], [14], [15], [16], with a brief survey in [17]. However, these abstraction methods are not based on any control-theoretic property of the network, nor do they answer quantitative questions such as “what system-theoretic information is lost when an abstraction is applied?”, or “how do the dynamics of the network model decide the level of abstraction”, etc.

In this paper we propose a new approach for fast design of RL controllers using the concept of dimensionality reduction. The basic idea is to exploit low-rank property of the controllability gramian of the system, project the measured states into a corresponding lower-dimensional space that captures the dominant eigenvectors of the gramian, and learn a LQR controller in this lower-dimensional space. Low-rank property of the controllability gramian in this case means that following a disturbance, one would need to control only the *dominantly controllable* behavior of the network states, and still be able to steer the network to its desired mission. Many practical systems that have lesser number of control inputs than states

¹ Department of Mechanical and Intelligent Systems Engineering, Graduate School of Informatics and Engineering, The University of Electro-Communications; 1-5-1, Chofugaoka, Chofu, Tokyo 182-8585, Japan. Email: sadamoto@uec.ac.jp

² Electrical & Computer Engineering, North Carolina State University; Raleigh, North Carolina, USA, 27695. Email: achakra2@ncsu.edu

³ Department of Systems and Control Engineering, Graduate School of Engineering, Tokyo Institute of Technology; 2-12-1, Oh-Okayama, Meguro, Tokyo, Japan. Email: imura@sc.e.titech.ac.jp

exhibit such low-rank controllability property. Common examples include consensus networks [18], heat diffusion networks [18], [19], electric power systems [20] and transportation networks [21], [22]. Especially in power system applications, several recent results have proposed the use of low-rank controllability for designing broadcast type controls, two leading examples being load-frequency control [23] and power oscillation damping [24]. Based on these observations, our proposed approach is to construct a matrix from online measurements of states and inputs that projects these measurements to a low-dimensional data space, capturing the dominant traits of the network dynamics. The matrix construction is done using singular value decomposition of the measurements. A RL controller is then designed based on this compressed data. Because of its lower dimensionality, the computational complexity for learning is drastically reduced. Stability and optimality of the control performance are theoretically evaluated using robust control theory by treating the dimensionality-reduction error as an uncertainty. The effectiveness of the proposed learning method is illustrated by numerical simulations.

A dimensionality-reduction based RL controller was recently proposed in [25] under the assumption that the network model exhibits a singular perturbation structure. This method is a special case of our approach when the projection matrix is known and is chosen to extract the slow-time-scale dynamics. Model-based control designs using dimensionality reduction have been proposed in earlier papers such as [26] as well as in more recent papers such as [27]. However, their extension to a completely model-free execution such as ours has not been reported yet. Our method is also superior to control designs that are based on system identification as in [28] as identification-based methods are indirect and so one cannot guarantee optimality even if full-dimensional system models are constructed. In contrast, our approach guarantees {suboptimality, optimality} when the dimensionality approximation error is {small, zero}.

The rest of the paper is organized as follows. Section II formulates the problem of fast RL control design, followed by Section III which presents an algorithm for this design assuming that the dimensionality reduction is exact. Theoretical results on closed-loop stability and performance degradation depending on the reduction error are derived in Section IV. An extension of the proposed algorithm to networks with semi-stable dynamics is presented in Section V, followed by numerical simulations in Section VI. Section VII concludes the paper.

Notation: We denote the set of real numbers as \mathbb{R} , the pseudo-inverse of a full-row rank matrix P as P^\dagger , the range space spanned by the column vectors of a matrix P as $\text{im}P$, the null space spanned by those as $\ker P$, and the n -dimensional identity matrix as I_n . The subscript n is omitted if obvious. We denote the i -th column vector of I_m as e_i^m , and the n -dimensional row vector whose entries are all one as $\mathbf{1}_n$. We denote a positive definite (semi-definite) matrix A as $A \succ 0$ ($A \succeq 0$). Given $P \in \mathbb{R}^{\hat{n} \times n}$ where $\hat{n} \leq n$, the matrix \bar{P} is defined such that $P^\dagger P + \bar{P}^\dagger \bar{P} = I$. When $\hat{n} = n$, \bar{P} is empty. The operator \otimes denotes the Kronecker product. For a matrix $P := [p_1, \dots, p_n]$, $\text{vec}(P) := [p_1^\top, \dots, p_n^\top]^\top$. For a

given Hurwitz $A \in \mathbb{R}^{n \times n}$ and $B \in \mathbb{R}^{n \times m}$, the controllability gramian is defined as $\Phi(A, B) := \int_0^\infty e^{At} B B^\top e^{A^\top t} dt$. When $\Phi(A, B)$ is full rank, the dynamical system $\dot{x} = Ax + Bu$ is said to be controllable. The Dirac-delta function is denoted as $\delta(t)$. The \mathcal{L}_2 -norm of a square integrable function $v(t) \in \mathbb{R}^n$ is defined by $\|v(t)\|_{\mathcal{L}_2} := \left(\int_0^\infty v^\top(t)v(t)dt\right)^{\frac{1}{2}}$. We denote the set of integrable function $v(t)$ satisfying $\|v(t)\|_{\mathcal{L}_2} \leq 1$ as $\mathcal{L}_2^{\text{nor}}$. The \mathcal{H}_∞ -norm of a stable proper transfer matrix $G(s)$ is defined by $\|G(s)\|_{\mathcal{H}_\infty} := \sup_{\omega \in \mathbb{R}} \|G(j\omega)\|$ where $\|\cdot\|$ denotes the induced 2-norm, and the \mathcal{H}_2 -norm of a stable strictly proper transfer matrix $G(s)$ is defined by $\|G(s)\|_{\mathcal{H}_2} := \left(\frac{1}{2\pi} \int_{-\infty}^\infty \text{tr}(G(j\omega)G^\top(-j\omega))d\omega\right)^{\frac{1}{2}}$.

II. PROBLEM SETUP

A. Brief Review of Off-Policy Iteration

Consider a linear networked dynamical system consisting of L subsystems. For $l \in \{1, \dots, L\}$, the l -th subsystem dynamics is described as

$$\Sigma_l: \dot{x}_{[l]} = A_{ll}x_{[l]} + \sum_{j \in \mathcal{N}_l} A_{lj}x_{[j]} + B_l u_{[l]}, \quad x_{[l]}(0) = x_{[l]0} \quad (1)$$

where $x_{[l]} \in \mathbb{R}^{n_l}$ is a state, $u_{[l]} \in \mathbb{R}^{m_l}$ is a control input, \mathcal{N}_l is the index set of subsystems connecting to the l -th subsystem, and $x_{[l]0}$ is an initial state of the subsystem. Using the notation

$$A := \begin{bmatrix} A_{11} & \cdots & A_{1L} \\ \vdots & \ddots & \vdots \\ A_{L1} & \cdots & A_{LL} \end{bmatrix}, \quad B := \begin{bmatrix} B_1 & & \\ & \ddots & \\ & & B_L \end{bmatrix} \\ n := \sum_{l=1}^L n_l, \quad m := \sum_{l=1}^L m_l, \\ x := [x_{[1]}^\top, \dots, x_{[L]}^\top]^\top, \quad u := [u_{[1]}^\top, \dots, u_{[L]}^\top]^\top, \quad (2)$$

the interconnected network model can be written as

$$\Sigma: \dot{x} = Ax + Bu, \quad x(0) = x_0. \quad (3)$$

We impose the following three assumptions on (3).

Assumption 1: The matrices A and B are unknown.

Assumption 2: The state x is measurable.

Assumption 3: The open-loop system in (3) is stable, i.e., A is Hurwitz.

Assumption 1 implies that although we know that the system of our interest is LTI we do not know its model. Even though many control systems in practice are nonlinear, their behavior can often be captured quite accurately by a linearized model around an operating point. In that case, this assumption implies that this linearized model is unknown, either because the original nonlinear model is unknown or because of other practical uncertainties. Assumptions 1-2 imply that both n and m are known. Assumption 3 is usually satisfied in many real-world networks where the underlying physical laws (Newton's law, Faraday's law, Kirchoff's law, etc.) ensure that the network dynamics are stable even if the network parameters are unknown. Our goal is to design a state-feedback controller

$$u = -Fx \quad (4)$$

such that the cost function

$$J := \int_0^\infty x^\top(t)Qx(t) + u^\top(t)Ru(t)dt \quad (5)$$

where $Q \succeq 0$ and $R \succ 0$ are chosen matrices, is minimized. If A and B were known one can find the optimal controller F in (4) by solving an algebraic Riccati equation [29]. However, since both of these matrices are completely unknown, the standard LQR approach no longer applies. Instead a reinforcement learning (RL) based approach needs to be used, as shown in recent papers such as [11], [30].

Several variants of RL exist in the literature. One popular method is known as policy iteration, which is further categorized into two approaches: on-policy and off-policy iteration [4], [11]. Both on- and off-policy iteration algorithms are equivalent to a data-driven implementation of the *Kleinman's Algorithm*, which is an iterative scheme to solve the algebraic Riccati equation associated with (5) [31]. At the k -th step of the on-policy iteration, under the assumption that a stabilizing control gain F_k is obtained, one updates the gain based on the data collected after applying the control law. This means that one has to recollect the data every time one updates the control law, resulting in a long learning time. Off-policy iteration, on the other hand, enables one-shot learning, i.e. one can find the optimal control gain by using only one set of data obtained before actuating the control signal. Because of its faster speed, we will be using off-policy iteration for developing our proposed RL controller. We next recapitulate the basic steps of the off-policy method.

The off-policy iteration consists of two stages, namely - *Online Data Collection* and *Policy Improvement*. In the first stage, one excites the system (3) with an exploration noise, say denoted as $u(t) = w(t)$ for $0 \leq t \leq 1$, $u(t) = 0$ for $t > 1$, and collects the time-series measurements of $x(t)$ driven by this noise and the initial state disturbance x_0 . In the second stage, one estimates the optimal control gain iteratively using the measured data. An overview of this estimation is as follows. Note that the open-loop system (3) can be rewritten as

$$\dot{x} = A_k x + Bu', \quad A_k := A + BF_k, \quad u' := u - F_k x \quad (6)$$

where F_k is a given stabilizing control gain, i.e., $A + BF_k$ is Hurwitz. This fictitious representation allows us to interpret the sequence $x(t)$ following the open-loop system (3) as the data of the closed-loop system (6) with an external signal u' . Given $\{t_j\}_{j=0}^N$, an incremental Lyapunov function candidate can be written as

$$\begin{aligned} & x^\top(t_{j+1})P_k x(t_{j+1}) - x^\top(t_j)P_k x(t_j) = \int_{t_j}^{t_{j+1}} \frac{d}{d\tau} x^\top(\tau)P_k x(\tau) d\tau \\ & = - \int_{t_j}^{t_{j+1}} x^\top(\tau)Q_k x(\tau) d\tau - 2 \int_{t_j}^{t_{j+1}} u'^\top(\tau)RF_{k+1}x(\tau) d\tau \quad (7) \end{aligned}$$

where $Q_k := Q + F_k^\top RF_k$. Note that (7) follows from the Kleinman's Algorithm. Because $x(t)$ in (7) follows from the open-loop system driven by the exploration noise $u(t)$, one only needs to collect $x(t)$ once for computing F_k . Once F_k converges, the final controller is implemented. The complete off-policy iteration algorithm is summarized in Algorithm 1.

Algorithm 1: Off-policy iteration [11]

Initialization:

Given N , $j \leftarrow 0$, $k \leftarrow 0$, $F_0 = 0$, $\kappa \geq 0$, fix a set $\{t_j\}_{j \in \{0, \dots, N\}}$ such that $t_N > \dots > t_0 \geq 0$.

Online Data Collection:

For $j = 0, \dots, N-1$, do:

1. Measure $x(t)$ for $t \in [t_j, t_{j+1}]$ under a given $u(t)$.
2. Numerically compute

$$\phi_j := (x(t_{j+1}) \otimes x(t_{j+1}) - x(t_j) \otimes x(t_j))^\top \in \mathbb{R}^{1 \times n^2} \quad (8)$$

$$\rho_j := \int_{t_j}^{t_{j+1}} (x(t) \otimes u(t))^\top dt \in \mathbb{R}^{1 \times nm} \quad (9)$$

$$\sigma_j := \int_{t_j}^{t_{j+1}} (x(t) \otimes x(t))^\top dt \in \mathbb{R}^{1 \times n^2} \quad (10)$$

Policy Improvement:

3. Find W_k and F_{k+1} satisfying

$$\Theta_k \begin{bmatrix} \text{vec}(W_k) \\ \text{vec}(F_{k+1}) \end{bmatrix} = z_k \quad (11)$$

with

$$\Theta_k := [\phi - 2\rho(I \otimes R) - 2\sigma(I \otimes F_k^\top R)] \in \mathbb{R}^{N \times (2n^2 + nm)} \quad (12)$$

$$z_k := -\sigma \text{vec}(Q + F_k^\top RF_k) \in \mathbb{R}^N \quad (13)$$

where $\phi \in \mathbb{R}^{N \times n^2}$, $\rho \in \mathbb{R}^{N \times nm}$, and $\sigma \in \mathbb{R}^{N \times n^2}$ are the stacked versions of ϕ_j , ρ_j , and σ_j , respectively.

4. Exit if $\|F_{k+1} - F_k\| \leq \kappa$, otherwise let $k \leftarrow k + 1$ and return to 3.
-

Note that (11) is the least-squares representation of (7). The following theorem from [11] shows that the off-policy iteration in Algorithm 1 produces an optimal controller.

Theorem 1: [11] Consider Σ in (3) and J in (5). Assume

$$\text{rank}[\rho \ \sigma] = \frac{n(n+1)}{2} + mn \quad (14)$$

where ρ and σ are the stacked vector representations of ρ_j in (9) and σ_j in (10). Then, the following two statements hold:

- i) $A - BF_k$ is Hurwitz for any integer $k > 0$, where F_k follows from the solution of (11).
- ii) Define $F_\infty := \lim_{k \rightarrow \infty} F_k$. The control $u = -F_\infty x$ minimizes J .

Since Algorithm 1 is equivalent to Kleinman's Algorithm [31], it can be easily derived that the iterates W_k are quadratically convergent. The main limitation of Algorithm 1 is that it is not easily scalable to high-dimensional networks with a large value of n . Step 3 of the algorithm is the main computational bottleneck. To solve (11), one needs to compute the pseudo-inverse of Θ_k in (12). The computational cost for that based on singular value decomposition is $\mathcal{O}(\min\{N^2 n^4, n^2 N^4\})$ [32], where N is the number of collected data samples. To satisfy (14), one must also have $N \geq \frac{n(n+1)}{2} + mn$, which makes the overall cost of the

algorithm $\mathcal{O}(n^6)$. Moreover, the pseudo-inverse must be computed at every iteration of the policy improvement. Thus, the *learning time*, defined as the time needed for running the Policy Improvement of Algorithm 1, may be unacceptably large, thereby limiting its application for real-time control.

B. Purpose and Approach of This Paper

Motivated by this problem, in this paper we propose an alternative approach for designing the model-free controller (4) such that it makes the cost function J in (5) as small as possible while reducing the learning time to significantly lesser than $\mathcal{O}(n^6)$. Our fundamental approach is to utilize the low-rank property of the controllability gramian of (3). In many large-scale network systems, disturbances and control inputs tend to excite only a part or a combination of the state variables [33], implying that the collected data $x(t)$ associated with a low-dimensional controllable subspace is sufficient for learning. As long as the data is compressed appropriately from the viewpoint of controllability, learning based on the low-dimensional data can be expected to work well. Our goal is to theoretically establish this intuition while at the same time developing an algorithm to learn F using low-dimensional data. The proposed approach is briefly summarized as follows:

- 1) First, we construct a reduced-dimensional compressed state vector ξ as

$$\xi := Px, \quad (15)$$

by projecting the measured state trajectory $x(t)$ through a full row-rank matrix $P \in \mathbb{R}^{\hat{n} \times n}$ where $\hat{n} \ll n$. The matrix P will capture the level of redundancy in the controllability of the network model (3) that allows for dimensionality reduction. Note that the system model is not known, so P will be constructed solely from the measurements of $x(t)$.

- 2) Next, a controller (4) is learned using the reduced-dimensional state $\xi(t)$ instead of the original state $x(t)$ such that the performance cost of the resulting closed-loop system is as close to the optimal cost J in (5) as possible.

In the following sections, we show how these steps are achieved.

III. PROPOSED ALGORITHM

A. A Sufficient Condition for Lossless Compression

We first consider an ideal situation when the data compression is lossless, i.e. $x(t)$ can be recovered from the compressed data $\xi(t)$. In that case, one can expect that the learning based on the lossless data $\xi(t)$ will provide an optimal controller minimizing J in (5). This is indeed true, as shown next. A sufficient condition for the lossless compression is to reduce the redundant states of x in terms of controllability. This is summarized as the following lemma.

Lemma 1: Consider Σ in (3). Let P satisfy

$$\text{im}P^\top = \text{im} \mathcal{R}(A, [B \ x_0]) \quad (16)$$

where $\mathcal{R}(A, b) := [b, Ab, \dots, A^{n-1}b]$. Then, ξ in (15) satisfies

$$\hat{\Sigma} : \dot{\xi} := PAP^\dagger \xi + PBu, \quad \xi(0) = Px_0, \quad (17)$$

where PAP^\dagger is Hurwitz. Furthermore,

$$x(t) \equiv P^\dagger \xi(t), \quad \forall t \quad (18)$$

holds for any $u(t)$ and x_0 .

Proof : See [34].

This lemma implies that if P satisfies (16), the \hat{n} -dimensional state ξ exactly captures the behavior of the n -dimensional state x . From (18), it follows that the cost function with respect to the compressed state ξ

$$\hat{J} := \int_0^\infty \xi^\top(t) \hat{Q} \xi(t) + u^\top(t) R u(t) dt, \quad \hat{Q} := (P^\dagger)^\top Q P^\dagger \quad (19)$$

is identical to J in (5). In other words, the learning for n -dimensional system Σ in (3) with a cost function J by using ξ is equivalent to the learning for the reduced-order system (17) with a cost function \hat{J} in (19). This can be done by employing the off-policy iteration method of Algorithm 1 if a matrix P satisfying (16) is found.

B. Construction of P from Data

We next show an approach by which one can construct P satisfying (16) by using the measured data $x(t)$ instead of the system model A and B . We first introduce the following lemma.

Lemma 2: Consider Σ in (3). If P satisfies (16), the condition

$$(I - P^\dagger P)x(t) \equiv 0, \quad \forall t \quad (20)$$

holds for any u and x_0 . In addition, without loss of generality, we suppose that \hat{n} is the minimal dimension for satisfying (20). Then, (20) is equivalent to (16).

Proof : First, we show the sufficiency. If (16) holds, by multiplying $\bar{P}^\dagger \bar{P}$ to (18) from the left, we have $\bar{P}^\dagger \bar{P} x(t) \equiv 0$ for any u, x_0, t . This is equivalent to (20). Next, we show (16) if (20) holds. To this end, we first show

$$P^\dagger P \mathcal{R}(A, [B \ x_0]) = \mathcal{R}(A, [B \ x_0]). \quad (21)$$

Note that (20) is assumed to be satisfied when $u = 0$. Thus, we have

$$P^\dagger P e^{At} x_0 = e^{At} x_0, \quad \forall t. \quad (22)$$

Substituting $t = 0$ in (22), we have $P^\dagger P x_0 = x_0$. Next, taking one time derivative of (22) and substituting $t = 0$, we have $P^\dagger P A x_0 = A x_0$. Repeating this procedure up to the $(n-1)$ -th order time-derivative, we have $P^\dagger P A^i x_0 = A^i x_0$ for $i \in \{0, \dots, n-1\}$. Next, consider an impulse input applied to the i -th control port, described as

$$u(t) = e_i^m \delta(t). \quad (23)$$

Note that $x(t)$ under this impulse input is $x(t) = e^{At}(x_0 + B_i)$. Thus, (20) can be written as

$$P^\dagger P e^{At}(x_0 + B_i) = e^{At}(x_0 + B_i), \quad \forall t,$$

where B_i denotes the i -th column of B . Substituting $t = 0$, we have $P^\dagger P B_i = B_i$, where the relation $P^\dagger P x_0 = x_0$ is used. Repeating the same procedure for all $i \in \{1, \dots, m\}$ and up to the $(n-1)$ -th order time-derivative, the relation (21) follows. Clearly, (21) is equivalent to $\text{im}P^\top \supseteq \text{im}\mathcal{R}(A, [B \ x_0])$. A minimal-dimensional P satisfying this relation yields $\text{im}P^\top = \text{im}\mathcal{R}(A, [B \ x_0])$, which is (16). This completes the proof. \square

Lemma 2 implies that P satisfying (20) spans a reachable subspace from u and x_0 . However, finding a P which satisfies (20) exactly for any arbitrary input signal u can be difficult. Therefore, we consider solving the following online minimization problem:

$$\min_{P \in \mathbb{R}^{\hat{n} \times n}} \sum_{j=0}^{N-1} \|(I - P^\dagger P)x(t_j)\|^2, \quad (24)$$

where $\hat{n} \leq n$ is a given design parameter, and $x(t_j)$ is the sampled state driven by initial state disturbance x_0 and an exploratory noise $u(t)$. The $x(t)$ measurements that are collected during the *Online Data Collection* step of Algorithm 1 can be used in (24) for finding P . One can see that the solution of (24) approximately satisfies (20) if N is sufficiently large. This minimization problem can be solved by using the singular value decomposition of

$$X := [x(t_0), \dots, x(t_{N-1})] \in \mathbb{R}^{n \times N}, \quad (25)$$

with P^\dagger given by the first \hat{n} columns of the left-singular matrix.

Another option can be to construct P offline, i.e., before the disturbance hits the network. This can further save online computation time. Offline construction of P , for example, can be done by using the *empirical controllability gramian* [35]. For $i \in \{1, \dots, m\}$, let $x_i(t)$ be the response of the system Σ in (3) with the impulse input given by (23). The empirical controllability gramian is defined as

$$\Phi_{\text{emp}}(t) := \sum_{i=1}^m \int_0^t (x_i(\tau) - \bar{x}_i(t)) (x_i(\tau) - \bar{x}_i(t))^\top d\tau \quad (26)$$

with $\bar{x}_i(t) := \frac{1}{t} \int_0^t x_i(\tau) d\tau$. It can be clearly seen that

$$\lim_{t \rightarrow \infty} \Phi_{\text{emp}}(t) = \Phi(A, B). \quad (27)$$

This implies that we can construct the controllability gramian by using m sets of $\{x(t), u(t)\}$ without knowing the system model. Although we do not know what disturbance is injected, it may be possible to know a possible subspace $\mathcal{X} \subseteq \mathbb{R}^n$ in which x_0 lies. In this situation, similarly as the above, we can construct another empirical controllability gramian associated with the disturbance. Let d_1, \dots, d_r be the basis of the distribution \mathcal{X} , i.e., $\text{im}[d_1, \dots, d_r] = \mathcal{X}$. Let $x_i(t)$ be the response of Σ with the disturbance of $x(0) = d_i$ for $i \in \{1, \dots, r\}$. Denote the empirical controllability gramian (26) by Φ_{emp}^x . Similarly, denote the gramian (26) associated with the input by Φ_{emp}^u . Then, by choosing eigenvectors of $\Phi_{\text{emp}} := \Phi_{\text{emp}}^u + \Phi_{\text{emp}}^x$ corresponding to the non-zero eigenvalues, we can construct P satisfying (21) for any $x_0 \in \mathcal{X}$.

C. Preconditioned Off-Policy Iteration

Based on the idea of constructing the projection matrix P from $x(t)$, and compressing x to ξ as described above, we are now ready to present our proposed RL control method. We refer to this method as *preconditioned* off-policy iteration. Unlike the regular off-policy iteration this method consists of three stages, namely - *Online Data Collection*, *Preconditioning*, and *Policy Improvement*. The first stage is identical to that in Algorithm 1. In the second stage, we define $\hat{\phi}$, $\hat{\rho}$, $\hat{\sigma}$ by replacing x in (8)-(10) with ξ . The revised matrices are computed as

$$\hat{\phi} = \phi(P^\top \otimes P^\top) \in \mathbb{R}^{1 \times \hat{n}^2} \quad (28)$$

$$\hat{\rho} = \rho(P^\top \otimes I) \in \mathbb{R}^{1 \times m\hat{n}} \quad (29)$$

$$\hat{\sigma} = \sigma(P^\top \otimes P^\top) \in \mathbb{R}^{1 \times \hat{n}^2} \quad (30)$$

The third stage is similar to the policy improvement stage of Algorithm 1, but the vector x is replaced with ξ by using the relation (18). The pseudo-code of the proposed algorithm is shown in **Algorithm 2**.

Algorithm 2: Preconditioned off-policy iteration

Initialization and Online Data Collection:

Same as in Algorithm 1.

Preconditioning:

1. Given \hat{n} , find P by SVD of (25).
2. Compute $\hat{\phi}$, $\hat{\rho}$, and $\hat{\sigma}$ in (28)-(30).

Policy Improvement:

3. Find \hat{W}_k and \hat{F}_{k+1} satisfying

$$\hat{\Theta}_k \begin{bmatrix} \text{vec}(\hat{W}_k) \\ \text{vec}(\hat{F}_{k+1}) \end{bmatrix} = \hat{z}_k \quad (31)$$

with

$$\Theta_k := \begin{bmatrix} \hat{\phi} & -2\hat{\rho}(I \otimes R) - 2\hat{\sigma}(I \otimes \hat{F}_k^\top R) \end{bmatrix} \in \mathbb{R}^{N \times (2\hat{n}^2 + \hat{n}m)} \quad (32)$$

$$\hat{z}_k := -\hat{\sigma} \text{vec}(\hat{Q} + \hat{F}_k^\top R \hat{F}_k) \in \mathbb{R}^N \quad (33)$$

where $\hat{\phi}$, $\hat{\rho}$, $\hat{\sigma}$ are defined as (28)-(30), and \hat{Q} is in (19).

4. Go to the next step if $\|\hat{F}_{k+1} - \hat{F}_k\| \leq \kappa$, otherwise, let $k \leftarrow k + 1$ and return to 3.
5. Return

$$F_k = \hat{F}_k P \quad (34)$$

Similar to Proposition 1, the convergence of Algorithm 2 and the optimality of the final controller are guaranteed as follows.

Theorem 2: Consider Σ in (3), and a P that satisfies (20). Assume

$$\text{rank}[\hat{\rho} \ \hat{\sigma}] = \frac{\hat{n}(\hat{n} + 1)}{2} + m\hat{n}, \quad (35)$$

where $\hat{\rho}$ and $\hat{\sigma}$ are defined in (29)-(30). If Algorithm 2 is applied to Σ , then the following two statements hold:

- i) $A - BF_k$ is Hurwitz for any integer $k > 0$, where F_k is given by (34).

ii) Define $F_\infty := \lim_{k \rightarrow \infty} F_k$. The control $u = -F_\infty x$ minimizes J in (5).

Proof : From the proof of Theorem 2.3.12 in [11], it follows that the control $u = -\hat{F}_k \xi$ stabilizes $\hat{\Sigma}$ in (17), i.e., $PAP^\dagger - PB\hat{F}_k$ is Hurwitz for any integer $k > 0$. Let $\bar{\xi} := \bar{P}x$. Applying the coordinate transformation from x to $[\xi^\top, \bar{\xi}^\top]^\top$, (3) is written as

$$\begin{bmatrix} \dot{\xi} \\ \dot{\bar{\xi}} \end{bmatrix} = \begin{bmatrix} PAP^\dagger & PAP^\dagger \bar{P} \\ 0 & \bar{P}A\bar{P}^\dagger \end{bmatrix} \begin{bmatrix} \xi \\ \bar{\xi} \end{bmatrix} + \begin{bmatrix} PB \\ 0 \end{bmatrix} u, \quad (36)$$

with $\xi(0) = Px_0$ and $\bar{\xi}(0) = 0$. Note that $\bar{P}B = 0$, $\bar{P}x_0 = 0$, and $\bar{P}A\bar{P}^\dagger = 0$ follow from (16). Since A is Hurwitz, from the upper-triangular structure of (36), $\bar{P}A\bar{P}^\dagger$ is also Hurwitz. Furthermore, since $PAP^\dagger - PB\hat{F}_k$ is Hurwitz, we can see that $A - BF_k$ is Hurwitz for any k . The claim i) follows from this. Furthermore, the control law $u = -\hat{F}_\infty \xi$ minimizes (19) subject to the dynamics (17). Finally, due to the uncontrollability of $\bar{\xi}$ as shown in (36) the control minimizes J in (5). This completes the proof. \square

The computational complexity of Algorithm 2 is significantly lower than that of Algorithm 1. Note that the left-singular eigenvectors of X are identical to those of XX^\top . The complexity of the preconditioning step is $\mathcal{O}(\max\{Nn, n^3\})$ where the first term is for computing XX^\top and the second is for finding P by the SVD of XX^\top [32]. In reality, the value of N for capturing the dominant controllable subspace will not be large; we will show this later in our numerical simulations. Methods such as [36] for computing dominant left-singular vectors can further reduce this computational cost. As mentioned in Section II-A, the computational cost for solving (32) is $\mathcal{O}(\hat{n}^6)$. Therefore, the overall computational complexity of Algorithm 2 is $\mathcal{O}(\max\{n^3, K\hat{n}^6\})$ where K is the number of iterations. Note that the value of K is also small because the policy improvement is quadratically convergent [31]. Thus, as long as \hat{n} is sufficiently small, Algorithm 2 will save a lot of learning time. This will be demonstrated through numerical simulations later.

IV. ROBUSTNESS ANALYSIS

In the previous section, we have assumed the matrix P to satisfy the condition (20). In reality, however, P obtained by solving (24) may not satisfy the condition exactly. Instead, one can only find a P that satisfies this condition approximately. Note that, since A is Hurwitz, for the obtained P there exists a positive number ϵ satisfying

$$\|(I - P^\dagger P)x(t)\|_{\mathcal{L}_2} \leq \epsilon. \quad (37)$$

for any $u \in \mathcal{L}_2^{\text{nor}}$ and a given x_0 . The following lemma is useful for analyzing the stability and the performance of the closed-loop system with a controller that is learned under this non-ideal condition.

Lemma 3: Consider Σ in (3), $\hat{\Sigma}$ in (17) and

$$\Delta : \begin{bmatrix} \dot{\hat{e}} \\ \dot{\hat{x}} \end{bmatrix} = \begin{bmatrix} PAP^\dagger & PAP^\dagger \bar{P} \\ 0 & A \end{bmatrix} \begin{bmatrix} \hat{e} \\ \hat{x} \end{bmatrix} + \begin{bmatrix} 0 \\ B \end{bmatrix} u \quad (38)$$

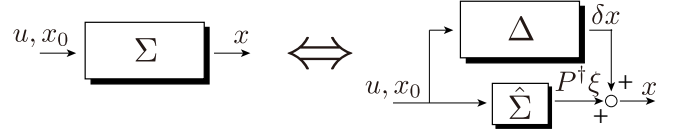


Fig. 1. Relation between Σ and the interconnection of $\hat{\Sigma}$ and Δ

with $\hat{e}(0) = 0$, $\hat{x}(0) = x_0$. The state x satisfies

$$x = P^\dagger \xi + \delta x, \quad \delta x := P^\dagger \hat{e} + \bar{P}^\dagger \bar{P} \hat{x} \quad (39)$$

where ξ obeys (17), for any $u(t)$ and $x_0 \in \mathbb{R}^n$.

Proof : Define

$$\begin{aligned} G(s) &:= (sI - A)^{-1}[B x_0] \\ \hat{G}(s) &:= P^\dagger (sI - PAP^\dagger)^{-1}[PB P x_0]. \end{aligned} \quad (40)$$

The state-space model of $\Delta(s) := G(s) - \hat{G}(s)$ is described as

$$\begin{cases} \begin{bmatrix} \dot{\hat{e}} \\ \dot{\hat{x}} \end{bmatrix} = \begin{bmatrix} PAP^\dagger & 0 \\ 0 & A \end{bmatrix} \begin{bmatrix} \hat{e} \\ \hat{x} \end{bmatrix} + \begin{bmatrix} PB & P x_0 \\ B & x_0 \end{bmatrix} \begin{bmatrix} u \\ \delta \end{bmatrix} \\ \delta x = -P^\dagger \hat{e} + \hat{x}. \end{cases} \quad (41)$$

Let $\hat{e} := P\hat{x} - \hat{\xi}$. Applying the coordinate transformation from $[\hat{\xi}^\top, \hat{x}^\top]^\top$ to $[\hat{e}^\top, \hat{x}^\top]^\top$, the system (41) is equivalently described as (38) with δx in (39). Since $G(s) = \Delta(s) + \hat{G}(s)$, the claim follows. \square

This lemma provides a tractable realization of Σ in the form of a parallel interconnection of the low-dimensional system $\hat{\Sigma}$ and the system Δ associated with the approximation error; see Fig. 1 for the signal-flow diagram of the interconnection. This parallel interconnection structure enables us to analyze the stability and performance of the closed-loop system using robust control theory. This is summarized as in the following theorem.

Theorem 3: Consider Σ in (3) and Algorithm 2. Let P be such that PAP^\dagger is Hurwitz. Let \hat{F}_k be the control gain at the k -th step of Algorithm 2. If

$$\epsilon < \|\hat{\Sigma}_{\text{cl}}(s)\Xi(s)\|_{\mathcal{H}_\infty}^{-1} \quad (42)$$

where ϵ follows from (37), and

$$\hat{\Sigma}_{\text{cl}}(s) := -\hat{F}_k (sI - \hat{A}_F)^{-1} PB\hat{F}_k - \hat{F}_k \quad (43)$$

$$\Xi(s) := P^\dagger (sI - PAP^\dagger)^{-1} PA \quad (44)$$

with $\hat{A}_F := PAP^\dagger - PB\hat{F}_k$, then, $A - BF_k$ is Hurwitz. Furthermore, there exists $\gamma \geq 0$ such that J in (5) satisfies

$$J^{\frac{1}{2}} \leq \hat{J}^{\frac{1}{2}} + \gamma \epsilon \quad (45)$$

where \hat{J} is defined in (19). When $\epsilon = 0$, $J = \hat{J}$.

Proof : We first prove the stability of the closed-loop system. Note that $Px = \xi + \hat{e}$ where \hat{e} is defined in (38). Thus, the interconnection of $\hat{\Sigma}$ with $u = -\hat{F}_k Px$ can be written as

$$\hat{\Sigma}_{\text{cl}} : \begin{cases} \dot{\hat{e}} = \hat{A}_F \hat{e} - PB\hat{F}_k \hat{e} \\ u = -\hat{F}_k \xi - \hat{F}_k \hat{e}. \end{cases} \quad (46)$$

The transfer function of $\Delta(s)$ in (38) from u to \hat{e} is

$$\Delta_{ue}(s) := P^\dagger (sI - PAP^\dagger)^{-1} PAP^\dagger \bar{P} (sI - A)^{-1} B. \quad (47)$$

Note

$$\begin{aligned} \|\hat{\Sigma}_{\text{cl}}\Delta_{ue}\|_{\mathcal{H}_\infty} &= \|\hat{\Sigma}_{\text{cl}}\Xi\bar{P}^\dagger\bar{P}(sI-A)^{-1}B\|_{\mathcal{H}_\infty} \\ &\leq \epsilon\|\hat{\Sigma}_{\text{cl}}\Xi\|_{\mathcal{H}_\infty} < 1. \end{aligned} \quad (48)$$

Thus, it follows from small-gain theorem that the closed-loop of $\hat{\Sigma}_{\text{cl}}$ and Δ_{ue} is stable.

Next, we analyze the performance achieved by the control $u = -F_k x$. Define $Q_{\frac{1}{2}}$ and $R_{\frac{1}{2}}$ as the respective Cholesky factors of Q and R , i.e., $Q_{\frac{1}{2}}^\top Q_{\frac{1}{2}} = Q$ and $R_{\frac{1}{2}}^\top R_{\frac{1}{2}} = R$. Define

$$y := \begin{bmatrix} Q_{\frac{1}{2}}x \\ R_{\frac{1}{2}}u \end{bmatrix}. \quad (49)$$

The closed-loop system can then be described as the interconnection of

$$\begin{cases} \dot{\xi} = \hat{A}_F\xi + B_\zeta\zeta + Px_0\delta \\ w = C_w\xi + D_{\xi\zeta}\zeta + D_{\xi\delta}\delta \\ y = C_y\xi + D_{y\zeta}\zeta \end{cases} \quad (50)$$

and Δ in (38), where $\zeta := [\hat{e}^\top, (\bar{P}^\dagger\bar{P}\hat{x})^\top]^\top$, $w := [u^\top, \delta]^\top$, and

$$\begin{aligned} B_\zeta &:= \begin{bmatrix} -PB\hat{F}_k & 0 \\ -F_k & 0 \\ 0 & 0 \end{bmatrix}, & C_w &:= [-F_k^\top & 0]^\top \\ D_{\xi\zeta} &:= \begin{bmatrix} 0 \\ 1 \end{bmatrix}, & D_{\xi\delta} &:= \begin{bmatrix} 0 \\ 1 \end{bmatrix} \\ C_y &:= \begin{bmatrix} Q_{\frac{1}{2}}P^\dagger \\ -R_{\frac{1}{2}}\hat{F}_k \end{bmatrix}, & D_{y\zeta} &:= \begin{bmatrix} Q_{\frac{1}{2}}\bar{P}^\dagger\bar{P} & Q_{\frac{1}{2}}P^\dagger \\ 0 & -R_{\frac{1}{2}}\hat{F}_k \end{bmatrix}. \end{aligned} \quad (51)$$

Thus

$$J^{\frac{1}{2}} = \|y\|_{\mathcal{L}_2} \leq \|G_{\delta y}\|_{\mathcal{H}_2} + \|G_{\zeta y}(I - \Delta G_{\zeta w})^{-1}\Delta G_{\delta w}\|_{\mathcal{H}_2} \quad (52)$$

where $G_{\bullet\bullet}$ denotes the transfer function of (51) from the input \bullet to the output \bullet , and Δ denotes that of the system (38) with the output ζ in (50). Note that $\|G_{\delta y}\|_{\mathcal{H}_2} = \hat{J}^{\frac{1}{2}}$ and

$$\begin{aligned} \Delta G_{\delta w} &= \begin{bmatrix} (sI - PAP^\dagger)^{-1}PA \\ I \end{bmatrix} \times \\ &\bar{P}^\dagger\bar{P}(sI - A)^{-1} \left(-B\hat{F}_k(sI - \hat{A}_F)^{-1}Px_0 + x_0 \right). \end{aligned} \quad (53)$$

From the sub-multiplicative property of the \mathcal{H}_∞ -norm, we get

$$\begin{aligned} J &\leq \hat{J}^{\frac{1}{2}} + \|\mathcal{G}(s)\|_{\mathcal{H}_\infty} \\ &\times \|\bar{P}^\dagger\bar{P}(sI - A)^{-1} \left(-B\hat{F}_k(sI - \hat{A}_F)^{-1}Px_0 + x_0 \right)\|_{\mathcal{H}_2} \end{aligned} \quad (54)$$

where

$$\mathcal{G}(s) := G_{\zeta y}(I - \Delta G_{\zeta w})^{-1}\Delta \begin{bmatrix} (sI - PAP^\dagger)^{-1}PA \\ I \end{bmatrix}.$$

Note that

$$\begin{aligned} &\|\bar{P}^\dagger\bar{P}(sI - A)^{-1} \left(-B\hat{F}_k(sI - \hat{A}_F)^{-1}Px_0 + x_0 \right)\|_{\mathcal{H}_2} \\ &\leq \|\bar{P}^\dagger\bar{P}(sI - A)^{-1}B\|_{\mathcal{H}_\infty} \|\hat{F}_k(sI - \hat{A}_F)^{-1}Px_0\|_{\mathcal{H}_2} \\ &+ \|\bar{P}^\dagger\bar{P}(sI - A)^{-1}x_0\|_{\mathcal{H}_2}. \end{aligned} \quad (55)$$

Now, we show that (37) yields

$$\|\bar{P}^\dagger\bar{P}(sI - A)^{-1}B\|_{\mathcal{H}_\infty} \leq 2\epsilon, \quad \|\bar{P}^\dagger\bar{P}(sI - A)^{-1}x_0\|_{\mathcal{H}_2} \leq \epsilon.$$

Let $x^{(x)}(t) := e^{At}x_0$ and $x^{(u)}(t) := \int_0^t e^{A(t-\tau)}Bu(\tau)d\tau$. Note that (37) holds for $u \equiv 0$. Thus, $\|\bar{P}^\dagger\bar{P}x^{(x)}\|_{\mathcal{L}_2} \leq \epsilon$, which implies $\|\bar{P}^\dagger\bar{P}(sI - A)^{-1}x_0\|_{\mathcal{H}_2} \leq \epsilon$. Since $x^{(u)} = x - x^{(x)}$, it follows that $\|\bar{P}^\dagger\bar{P}x^{(u)}\|_{\mathcal{L}_2} \leq \|\bar{P}^\dagger\bar{P}x\|_{\mathcal{L}_2} + \|\bar{P}^\dagger\bar{P}x^{(x)}\|_{\mathcal{L}_2} \leq 2\epsilon$ for any $u \in \mathcal{L}_2^{\text{nor}}$. This is equivalent to $\|\bar{P}^\dagger\bar{P}(sI - A)^{-1}B\|_{\mathcal{H}_\infty} \leq 2\epsilon$. From (54) and (55), (45) follows where

$$\gamma := \|\mathcal{G}(s)\|_{\mathcal{H}_\infty} (1 + 2\|\hat{F}_k(sI - \hat{A}_F)^{-1}Px_0\|_{\mathcal{H}_2}). \quad (56)$$

This completes the proof. \square

We briefly discuss a set of situations where (42) holds and PAP^\dagger is Hurwitz. In general, PAP^\dagger tends to be stable as \hat{n} gets larger because A is Hurwitz. Moreover, it is known that PAP^\dagger is always stable for $A = A^\top$ (e.g., bidirectional networks composed of first-order subsystems) [37] or for A as Metzler (e.g., positive directed networks) [38]. Note here that $P^\dagger = P^\top$ holds if P is chosen by left-singular vectors of X in (25). Similarly, it is clear from (43) that $\|\hat{\Sigma}_{\text{cl}}\|_{\mathcal{H}_\infty}$ gets smaller as $\|\hat{F}_k\|$ is smaller. Thus, from (48) and the fact $\|\hat{\Sigma}_{\text{cl}}\Xi\|_{\mathcal{H}_\infty} \leq \|\hat{\Sigma}_{\text{cl}}\|_{\mathcal{H}_\infty}\|\Xi\|_{\mathcal{H}_\infty}$, we can see that (42) holds for low-gain controllers, which can be achieved by choosing the input weight R in (5) to be large. Using a low-gain controller, however, may result in a poor \hat{J} . This can be counteracted by choosing a P that makes the approximation error ϵ in (37) small, thereby improving the ideal cost \hat{J} .

When these assumptions are satisfied, Theorem 3 implies the following two results: first, the learned controller at the k -th step of Policy Improvement in Algorithm 2 guarantees the stability of the closed-loop system. Second, smaller this error closer is the closed-loop performance cost to the ideal cost \hat{J} .

V. EXTENSION TO SEMI-STABLE SYSTEMS

We next extend Algorithm 2 to semi-stable systems. For simplicity of analysis, we assume that A in system (3), although unknown, has one semi-stable eigenvalue. This is often the case when the network exhibits a consensus property over a connected graph [39]. The proposed approach can be easily generalized to systems with multiple semi-stable poles. We denote the eigenvector associated with the semi-stable pole as v . The main assumption behind the proposed method is that v must be known. This assumption is actually true for many real-world applications. For consensus networks, v is the vector of all ones. For power system networks, where the semi-stable pole arises from Kirchoff's current balance, v contains identical entries corresponding to the generator phase angles while all other entries are zero. This is because the dynamics of the generators are coupled through the difference of their phase angles, and therefore the eigenvector v that changes all the angles uniformly does not have any influence on the dynamics. Moreover in many of these networks the control objective is driven by the goal of controlling relative states to quantify how one agent is performing with respect to another. In such situations, a common assumption that is satisfied is:

$$\ker Q \supseteq \text{im } v. \quad (57)$$

Starting from these observations, we state the following proposition.

Proposition 1: Consider a semi-stable system Σ in (3), whose semi-stable eigenvector is denoted by v . Construct $P_c \in \mathbb{R}^{\hat{n} \times (n-1)}$ such that

$$(I - P_c^\dagger P_c) \bar{v}^\dagger x(t) \equiv 0, \quad \forall t \quad (58)$$

for any u and a fixed x_0 . Define

$$P = P_c \bar{v}^\dagger. \quad (59)$$

Suppose that (35) is satisfied. If Q in (5) satisfies (57), then by applying Algorithm 2 to the semi-stable system Σ the following two statements hold:

- i) $A - BF_k$ is semi-stable whose semi-stable eigenvector is v .
- ii) The control $u = -F_\infty x$ minimizes J in (5).

Proof : Define $\eta := v^\dagger x$ and $\bar{\eta} := \bar{v}^\dagger x$. Applying a coordinate transformation from x to $[\bar{\eta}^\top, \eta^\top]^\top$, we have

$$\begin{bmatrix} \dot{\bar{\eta}} \\ \dot{\eta} \end{bmatrix} = \begin{bmatrix} \bar{v}^\dagger A \bar{v} & 0 \\ v^\dagger A \bar{v} & 0 \end{bmatrix} \begin{bmatrix} \bar{\eta} \\ \eta \end{bmatrix} + \begin{bmatrix} \bar{v}^\dagger B \\ v^\dagger B \end{bmatrix} u, \quad (60)$$

where the relation $Av = 0$ is used. Note that $\bar{v}^\dagger A \bar{v}$ is Hurwitz. Similar to Lemma 1, it follows that

$$\text{im} P^\top = \text{im} \mathcal{R}(\bar{v}^\dagger A \bar{v}, \bar{v}^\dagger [B \ x_0]).$$

Therefore, applying coordinate transformation from $\bar{\eta}$ to $[\xi^\top, \bar{\xi}^\top]^\top$ where $\bar{\xi} := \bar{P}x$, we get (17). The compressed state ξ obeys (17). From the upper-triangular structure of (36) and the fact that (36) is stable, we can see that PAP^\dagger is Hurwitz. Furthermore, we denote the Cholesky factor of Q by $Q_{\frac{1}{2}}$, i.e., $Q = Q_{\frac{1}{2}}^\top Q_{\frac{1}{2}}$. Since (57) yields $Q_{\frac{1}{2}} v = 0$, we have

$$Q_{\frac{1}{2}} x = Q_{\frac{1}{2}} (\bar{v} \bar{\eta} + v \eta) = Q_{\frac{1}{2}} \bar{v} (P_c^\dagger \xi + \bar{P}_c^\dagger \bar{\xi}) = Q_{\frac{1}{2}} P^\dagger \xi,$$

where the relation $\bar{\xi}(t) \equiv 0$ is used. Thus, $x^\top Q x = \xi^\top \hat{Q} \xi$. Similar to the proof of Theorem 1, it is proven that $PAP^\dagger - PB\hat{F}_k$ is Hurwitz for any k . Note that the eigenvalues of $A - BF_k$ with F_k in (34) are identical to those of $PAP^\dagger - PB\hat{F}_k$, $\bar{P}A\bar{P}^\dagger$, plus a zero eigenvalue. Thus, $A - BF_k$ is semi-stable. Also note that

$$(A - BF_k)v = -B\hat{F}_k P_c \bar{v}^\dagger v = 0.$$

Thus, v is the eigenvector corresponding to the semi-stable pole of $A - BF_k$. Therefore, claim i) follows. Claim ii) follows by using the same argument as in the proof of Theorem 1. This completes the proof. \square

This proposition implies that as long as P_c satisfies (58), i.e. the data compression is lossless, Algorithm 2 with P defined in (59) can provide an optimal controller for semi-stable systems. Such a matrix P_c can be found by the singular value decomposition of

$$X_c = \bar{v} X$$

where X is defined in (25). Furthermore, even for the non-ideal case when $\|(I - P_c^\dagger P_c) \bar{v}^\dagger x(t)\| \leq \epsilon$, Theorem 3 with P defined in (59) still holds for semi-stable systems.

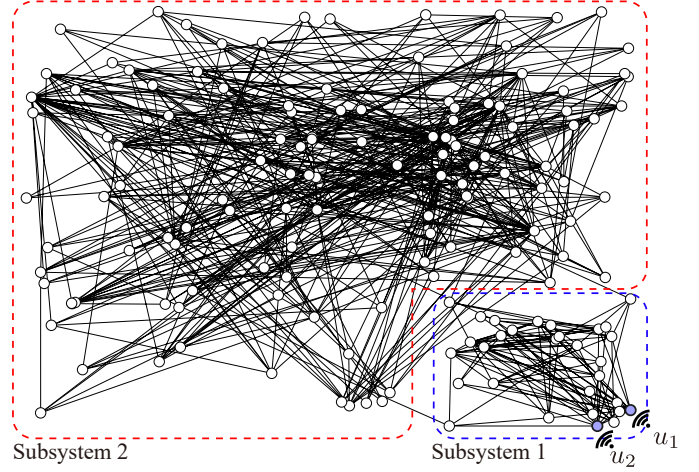


Fig. 2. A consensus network system composed of 150 nodes

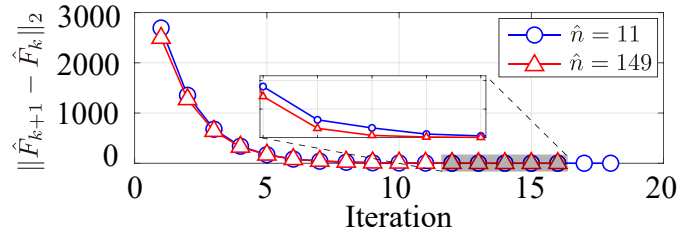


Fig. 3. The variation of the change of \hat{F}

VI. NUMERICAL SIMULATION

A. Case 1: Consensus Network System

We investigate the effectiveness of the proposed algorithm through an example of a consensus network as shown in Fig. 2. The network is composed of two subsystems (areas) consisting of 30 and 120 nodes, respectively. The fact that the network consists of two areas is only used for describing the network structure and its dynamics. We will not utilize this fact for controller design. The dynamics of the i -th node is described as

$$\dot{x}_i = \sum_{j \in \mathbb{N}_i} a_{i,j} (x_j - x_i) + b_i u_i, \quad (61)$$

where $x_i \in \mathbb{R}$ is the state, and \mathbb{N}_i is the index set of nodes connected to the i -th node. The inter-area graph structure is given as a Barabasi-Albert model [40], and the weights of the edges are randomly chosen from the range $(0, 0.5]$. The two areas are connected through four links between four nodes in each area. The link weights are all assigned to be 0.1. Let control inputs be applied only to the first two nodes of Area 1, i.e., $b_1 = b_2 = 1$ and $b_i = 0$ for $i \in \{3, \dots, 150\}$. Clearly, the system (61) can be described as (3) with $n = 150$. Note that this network system is semi-stable, and the corresponding eigenvector is $\mathbf{1}_n$.

The control objective here is to improve the speed of consensus among all nodes without knowing $a_{i,j}$ and b_i for all $\{i, j\}$. To this end, we take Q in (5) such that $x^\top Q x = \alpha \sum_{i=1}^n (x_i - x_i)^2$ with a scalar weight α , and $R = I$. Let $\alpha = 50$. The sampling sequence $\{t_j\}$ in the *Online Data Collection* stage is taken as $t_j = 0.01j$ for

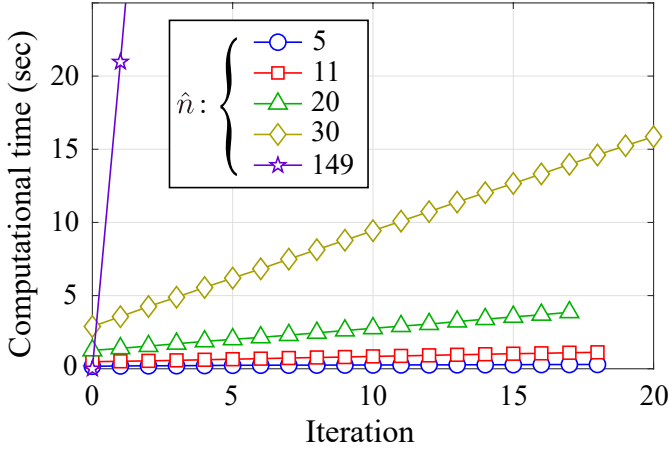


Fig. 4. Computational time needed for controller design

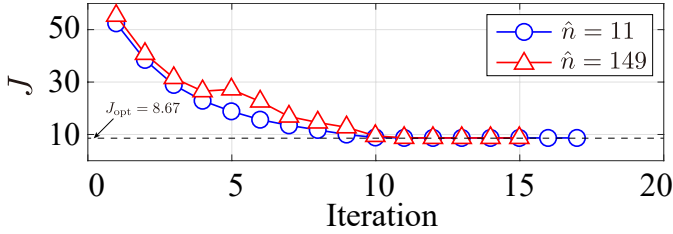


Fig. 5. The variation of the performance as the increase of iteration, where J_{opt} is the cost achieved by the model-based optimal controller.

$j \in \{0, \dots, 2000\}$. From $t = 0$ to $t = 1$ (sec), we inject the noise $u(t) = \beta \sum_{k=1}^{400} \sin(w_k t)$ with w_k randomly chosen from the range $[-20, 20]$ for $k \in \{1, \dots, 400\}$. Let $\beta = 0.05$.

We first find P as given in (59), by using the collected data $\{x(t_j)\}_{j \in \{0, \dots, 2000\}}$. Since the consensus network system is semi-stable, we project the data onto the stable subspace. Let $\bar{v}^\dagger \in \mathbb{R}^{(n-1) \times n}$ be such that $\bar{v}^\dagger \mathbf{1}_n = 0$. We compute $\bar{\eta} = \bar{v}^\dagger x$. Next, similarly to (24), for a given \hat{n} we solve $\min_{P_c \in \mathbb{R}^{\hat{n} \times (n-1)}} \sum_{j=0}^{N-1} \|(I - P_c^\dagger P_c) \bar{\eta}^\dagger(t_j)\|^2$. Let $\hat{n} = 11$. We conclude the preconditioning step in Algorithm 2 by computing $\hat{\phi}$, $\hat{\rho}$, and $\hat{\sigma}$ in (28)-(30). The state-feedback gain \hat{F}_k is computed by running the Policy Improvement step. Fig. 3 shows the variation of \hat{F}_k in (31) for $\hat{n} = 11$ and 149. Under the criterion that the algorithm is stopped when $\|\hat{F}_{k+1} - \hat{F}_k\| \leq 0.01$, it takes 16 iterations to converge when $\hat{n} = 11$, and 18 when $\hat{n} = 149$. In other words, the convergence speed for $\hat{n} = 11$ is almost the same as that for $\hat{n} = 149$. Furthermore, the resultant control performance for $\hat{n} = 11$ is $J = 8.70$ while that achieved by the optimal model-based controller is $J_{\text{opt}} = 8.67$. This result shows that the obtained controller for $\hat{n} = 11$ achieves nearly optimal control performance.

Next, we investigate the computational complexity of Algorithm 2. All computations were done using MATLAB 2017b, in an Intel(R) Core(TM) i7-4587U 3.00GHz, RAM 16.0GB computer. Fig. 4 shows the computational time taken for the Policy Improvement portion of Algorithm 2, for different values of \hat{n} . The computational time at the initial iteration is the time used for preconditioning. The purple line with stars corresponds to the case where Algorithm 1 without data

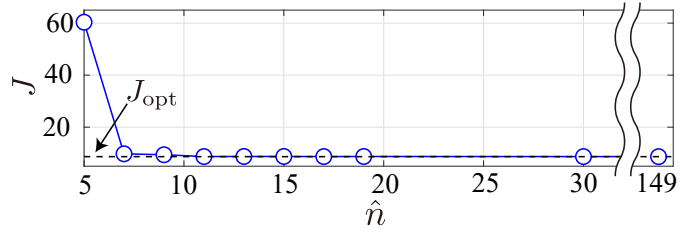


Fig. 6. Cost versus the dimensionality

w/o control	With control in case where $\hat{n} = 11$	With F_{opt}
0.0000	0.0000	0.0000
-0.0127	-0.2631	-0.2615
-0.2735	-0.2991	-0.2787
-0.2958	-0.3770	-0.3396
-0.3769	-0.4022	-0.3769

TABLE I

FIRST FIVE DOMINANT EIGENVALUES OF THE OPEN-LOOP SYSTEM AND CLOSED-LOOP SYSTEM

compression is applied, i.e., $P_c = I$. The line shows that as high as 21 seconds of real-time are needed for each step of Policy Improvement. On the other hand, the blue, red, green, and yellow lines with circles, squares, triangles, and diamonds show the case for different values of $\hat{n} \leq n$. By comparing those with the purple line, we can see that the dimensionality reduction efficiently reduces the computational time at every step. For example, the total computation time without data compression is 337 seconds whereas that with reduction of $\hat{n} = 20$ is only 4 seconds. Fig. 5 shows the convergence of the performance objective J for $\hat{n} = 11$ and 149. In both cases at least 10 iterations are needed for achieving nearly optimal control performance. On the other hand, the computational time for $\hat{n} = 149$ is 175 seconds while that for $\hat{n} = 11$ is only 0.6 seconds. These results confirm that the data compression drastically reduces the learning time.

Fig. 6 shows the cost J for different choice of controllers learned for different values of \hat{n} . From this figure, we can see that there exists a trade-off relation between the dimensionality (i.e., computational time) and closed-loop performance. For comparison, we design an optimal controller gain F_{opt} by solving a Riccati equation for the original system model (3). In Fig. 6, the dashed line shows the cost J_{opt} achieved by this ideal controller. We can see that the controller with $\hat{n} = 11$ is almost optimal. Furthermore, Table VI-A shows the first five dominant eigenvalues of the open-loop system and the closed-loop system when $F_{18} = \hat{F}_{18}P$ and F_{opt} are used, respectively. Clearly, the second dominant eigenvalue, associated with the consensus speed, is drastically improved by the proposed RL controller.

We close this subsection by investigating how the matrix P obtained by solving (24) approximates the ideal relation (20). One choice of ϵ satisfying (37) is given as

$$\epsilon := \|\bar{P}^\dagger \bar{P}(sI - A)^{-1} B\|_{\mathcal{H}_\infty} + \|\bar{P}^\dagger \bar{P}(sI - A)^{-1} x_0\|_{\mathcal{H}_2} \quad (62)$$

where P is constructed from (24). Clearly, the condition (20) is equivalent to (37) with $\epsilon = 0$. Thus, the parameter ϵ in (62) can be a measure that can quantify how accurately P in (24) approximates (20). Considering that $\{x(t_j)\}_{j \in \{0, \dots, 2000\}}$

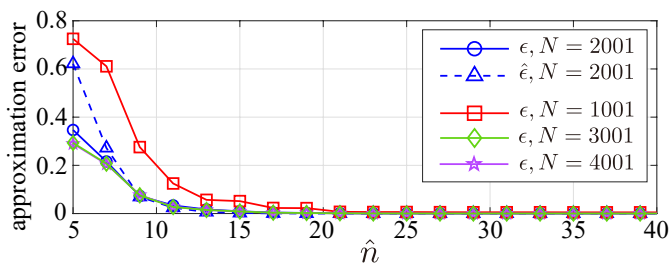


Fig. 7. The approximation error ϵ in (62) versus \hat{n}

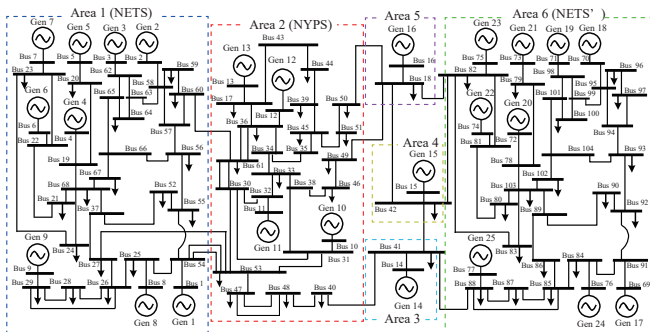


Fig. 8. Power system model consisting of 25 generators, 52 loads, and 104 buses.

(i.e., $N = 2001$) is used for formulating (24), we compute ϵ for different choices of \hat{n} . In Fig. 7, the blue line with circles show the resultant ϵ for \hat{n} . We can see that the value of ϵ in (62) becomes smaller as \hat{n} increases. Moreover, when $\hat{n} = 29$, the resultant $\epsilon = 1.5 \times 10^{-4}$, which implies that the obtained P in this case is almost ideal. This tendency is also observed when the endpoint of the sampling index j is changed to 1000, or 3000, or 4000. Furthermore, we can see that the variation of ϵ over \hat{n} saturates after a certain point as N increases. This is because the original controllable subspace $\mathcal{R}(A, [B, x_0])$ is fixed and the controllable subspace captured by the data becomes closer to the original as N increases. The exact value of ϵ is, however, difficult to compute using only the acquired data $\{x_j\}$ because A and B are unknown. One alternative metric instead of ϵ in (62) can be

$$\hat{\epsilon} := \sqrt{\text{tr}((\bar{P}^\dagger)^\top X \bar{P})} \quad (63)$$

where X is defined in (25). The reason why this can be an alternative is that when the input u is white Gaussian and $x_0 = 0$, as N increases we can expect that the value $\hat{\epsilon}$ converges to $\|\bar{P}^\dagger \bar{P} x\|_{\mathcal{L}_2}$. In Fig. 7, we show $\hat{\epsilon}$ by the red line with triangles. By comparing this and the blue line, we can see that indeed $\hat{\epsilon}$ in (63) can be a guideline for choosing \hat{n} .

B. Case 2: Power System Model

Next, we investigate how the proposed reinforcement learning controller can be effectively applied for wide-area oscillation damping of an electric power system without the knowledge of its small-signal model. We consider a power system model composed of six areas, as shown in Fig. 8. Note that these areas need not be coherent. The part containing areas 1 through 5 is the standard IEEE 68-bus model [41],

while Area 6 is a repetition of Area 1. This area models the New England test system (NETS). The overall model consists of 25 synchronous generators and 52 loads, interconnected via 104 buses. The loads are modeled as constant impedance loads. Following [42], the dynamics of the power system can be modeled as a nonlinear differential-algebraic equation

$$\dot{x} = f(x, V, w), \quad 0 = g(x, V) \quad (64)$$

where $x := [x_1^\top, \dots, x_{25}^\top]^\top \in \mathbb{R}^{100}$, $x_k \in \mathbb{R}^4$ is the state of the k -th generator (angle, frequency deviation, internal voltage, and field voltage), $V := [V_1, \dots, V_{104}]^\top \in \mathbb{C}^{104}$, V_k is the complex-valued voltage of the k -th bus, $w := [w_1, \dots, w_{25}]^\top \in \mathbb{R}^{25}$ and $w_k \in \mathbb{R}$ is the control input which enters the automatic voltage regulator (AVR) as an additional reference voltage signal to the k -th generator. We suppose that the state x is available from state estimators based on Phasor Measurement Units (for details please see [43]). Due to the double integrator in the swing equations, the small-signal model corresponding to (64) is semi-stable, with the eigenvector for the zero eigenvalue being $v = \mathbf{1}_{25} \otimes e_1^4$. We consider a fault, which is modeled as an impulse input reflected through the change in the initial conditions of the states from their pre-disturbance equilibrium. The frequency deviations of generators in Areas 1-6 after this fault are depicted by the blue, red, cyan, yellow, purple, and green lines in Fig. 9(a), respectively. We can see from this subfigure that the inter-area oscillations (whose frequency lies in the range 0.1-2.0 Hz) appear dominantly in the time-responses of the generator frequencies. To enhance the damping performance of this power system, we consider designing a model-free reinforcement learning controller. Although the controller is designed based on a linearized model, it is implemented using the original nonlinear model (64).

We consider that the control input of every generator inside the l -th area, where $l \in \{1, \dots, 6\}$, is equal. That is, $w_i = u_{[l]}$ for any i in the index set of the generators belonging to the l -th area. Let $u = [u_{[1]}, \dots, u_{[6]}]^\top$. The control input is determined by

$$u = F(x - x^*) \quad (65)$$

where x^* is the setpoint of x in (64). Note that this setpoint is a priori known by measuring the steady state without exploiting any detailed knowledge about the system model. The controller gain F is determined from Algorithm 2 replacing x with $x - x^*$. The design parameters are chosen as follows. Q in (5) is chosen such that $x^\top Q x = \alpha \sum_{l=1}^6 \omega_{[l]}^2$ where $\omega_{[l]}$ is the average frequency deviation of generators inside the l -th area and α is a scalar weight. We choose $\alpha = 10$ and $R = I$ in (5). From $t = 0$ to $t = 2$ (sec), we inject the exploration noise described in VI-A to each generator through its excitation system voltage w_k . The noise amplitude is taken as $\beta = 10^{-3}$. The data is collected for time $t \in [0, 18]$ with a sampling period of 0.01 seconds. The total time for executing Algorithm 1 is found to be 140.4 seconds. The designed controller is implemented in the system starting from time $t = 18 + 140.4 = 158.4$ (sec). Fig. 9(b) shows the trajectories of the frequency deviations of all generators after the implementation of the controller. By comparing Figs. 9(a)

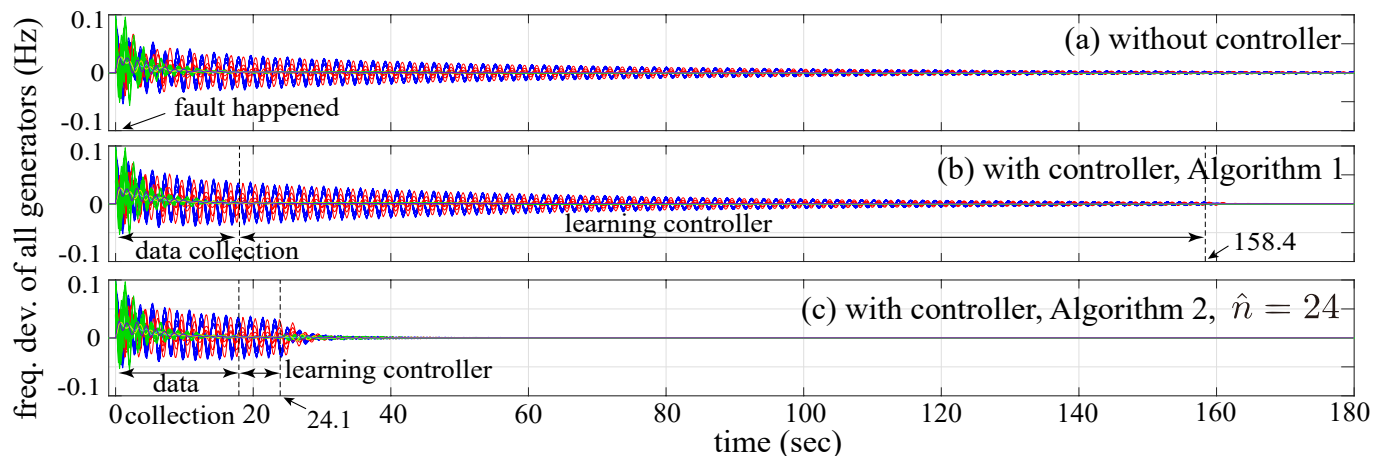


Fig. 9. Transient response of frequency deviation of generators (a) without control, (b) by the optimal controller designed by Algorithm 1, and (c) by the proposed controller in Algorithm 2.

and (b), one can see that the damping performance over the entire time-horizon of interest is very limited due to the long learning time (140.4 seconds). To reduce the computation time, we apply the Algorithm 2 to the system with $\hat{n} = 24$. The learning time in that case reduces to only 6.1 seconds. Fig 9(c) shows the case where the designed controller is implemented at time $t = 24.1$ (sec). It can be clearly seen that the performance improves drastically compared to Figs. 9(a)-(b). Note that the controller is linear while the power system model used for the simulations is described by the nonlinear model (64). This demonstrates the inherent robustness property of the proposed RL controller for this example.

VII. CONCLUSION

In this paper, we proposed a new RL control strategy for large-scale network systems. The proposed control strategy can avoid the curse of dimensionality by utilizing the low-rank property of the network in terms of its controllability. In the proposed strategy, (almost) uncontrollable state variables are eliminated by projecting the state data on to the controllable subspace. This projection is achieved in a completely model-free way using only measured data. Results are validated by two practical examples, both of which show notable speed-up of the learning time while guaranteeing satisfactory sub-optimal performance. The main contribution of the paper is to show how two individually well-known concepts in dynamical system theory and machine learning - namely, model reduction and reinforcement learning - can be combined together to construct a real-time control design that can be highly useful for extreme-scale networks. We have shown a trade-off relation between the improvement of learning time and the cost of degradation of the closed-loop performance due to the data compression error, answering the two questions that were raised in the introduction.

Our future work will include the extension of this method to a hierarchical structure where microscopic or local controllers and macroscopic or global controllers are learned in parallel using the data compression concept. We also wish to extend this approach to a stochastic setting using discrete-time

Markov decision processes (MDPs), and to nonlinear input-affine systems as the recent paper [44] shows that the SVD of the matrix X in (25) can capture the controllable subspace of such nonlinear systems.

ACKNOWLEDGMENT

This research was partially supported by CREST, JST Grant Number JPMJCR15K1, Japan. The work of the first author was partly supported by JSPS Grant-in-Aid for Research Activity Start-up JP19K2350.

REFERENCES

- [1] K. S. Narendra and K. Parthasarathy, "Identification and control of dynamical systems using neural networks," *IEEE Transactions on neural networks*, vol. 1, no. 1, pp. 4–27, 1990.
- [2] P. J. Werbos, "Neural networks for control and system identification," in *Proc. of Conference on Decision and Control*, 1989, pp. 260–265.
- [3] M. Vidyasagar and R. L. Karandikar, "A learning theory approach to system identification and stochastic adaptive control," *Journal of Process Control*, vol. 18, no. 3–4, pp. 421–430, 2008.
- [4] R. S. Sutton and A. G. Barto, *Reinforcement learning: An introduction (Second Edition)*. The MIT Press, 2011.
- [5] F. L. Lewis and D. Vrabie, "Reinforcement learning and adaptive dynamic programming for feedback control," *IEEE circuits and systems magazine*, vol. 9, no. 3, pp. 32–50, 2009.
- [6] P. Mehta and S. Meyn, "Q-learning and pontryagin's minimum principle," in *Proc. of Conference on Decision and Control*, 2009, pp. 3598–3605.
- [7] P. P. Khargonekar and M. A. Dahleh, "Advancing systems and control research in the era of ML and AI," *Annual Reviews in Control*, vol. 45, pp. 1–4, 2018.
- [8] B. Recht, "A tour of reinforcement learning: The view from continuous control," *arXiv preprint arXiv:1806.09460*, 2018.
- [9] Q. Wei, D. Liu, and H. Lin, "Value iteration adaptive dynamic programming for optimal control of discrete-time nonlinear systems," *IEEE Transactions on cybernetics*, vol. 46, no. 3, pp. 840–853, 2015.
- [10] D. P. Bertsekas, *Dynamic programming and optimal control*. Athena scientific Belmont, 1995.
- [11] Y. Jiang and Z. Jiang, *Robust adaptive dynamic programming*. Wiley IEEE Press, 2017.
- [12] —, "Robust adaptive dynamic programming for large-scale systems with an application to multimachine power systems," *IEEE Transactions on Circuits and Systems*, vol. 59, no. 10, pp. 693–697, 2012.
- [13] J. N. Tsitsiklis and B. Van Roy, "Feature-based methods for large scale dynamic programming," *Machine Learning*, vol. 22, no. 1-3, pp. 59–94, 1996.

- [14] S. P. Singh, T. Jaakkola, and M. I. Jordan, "Reinforcement learning with soft state aggregation," in *Proc. of Advances in neural information processing systems*, 1995, pp. 361–368.
- [15] S. Lin and R. Wright, "Evolutionary tile coding: An automated state abstraction algorithm for reinforcement learning," in *Proc. of Workshops at the Twenty-Fourth AAAI Conference on Artificial Intelligence*, 2010, pp. 43–47.
- [16] D. Abel, D. E. Hershkowitz, and M. L. Littman, "Near optimal behavior via approximate state abstraction," *arXiv preprint arXiv:1701.04113*, 2017.
- [17] L. Li, T. J. Walsh, and M. L. Littman, "Towards a unified theory of state abstraction for MDPs," in *Proc. of International Symposium on Artificial Intelligence and Mathematics*, 2006, pp. 531–539.
- [18] T. Sadamoto, T. Ishizaki, and J. Imura, "Average state observers for large-scale network systems," *IEEE Transactions on Control of Network Systems*, vol. 4, no. 4, pp. 761–769, 2016.
- [19] T. Sadamoto, K. Kashima, H. Morita, and H. Mizuno, "Nonlinear reduced order modeling of plasticization cylinders," in *Proc. of American Control Conference*, 2014, pp. 129–134.
- [20] J. H. Chow, *Power system coherency and model reduction*. Springer, 2013, vol. 84.
- [21] J. S. Niedbalski, K. Deng, P. G. Mehta, and S. Meyn, "Model reduction for reduced order estimation in traffic models," in *Proc. of American Control Conference*, 2008, pp. 914–919.
- [22] S. P. Hoogendoorn and P. H. Bovy, "State-of-the-art of vehicular traffic flow modelling," *Proc. of the Institution of Mechanical Engineers, Part I: Journal of Systems and Control Engineering*, vol. 215, no. 4, pp. 283–303, 2001.
- [23] H. Shayeghi, H. Shayanfar, and A. Jalili, "Load frequency control strategies: A state-of-the-art survey for the researcher," *Energy Conversion and management*, vol. 50, no. 2, pp. 344–353, 2009.
- [24] N. Xue and A. Chakraborty, "Control inversion: A clustering-based method for distributed wide-area control of power systems," *IEEE Transactions on Control of Network Systems*, vol. 6, no. 3, pp. 937–949, 2019.
- [25] S. Mukherjee, H. Bai, and A. Chakraborty, "On model-free reinforcement learning of reduced-order optimal control for singularly perturbed systems," in *Proc. of Conference on Decision and Control*, 2018, pp. 5288–5293.
- [26] P. Kokotovic, H. K. Khali, and J. O'reilly, *Singular perturbation methods in control: analysis and design*. Siam, 1999, vol. 25.
- [27] N. Xue and A. Chakraborty, "Optimal control of large-scale networks using clustering based projections," *arXiv preprint arXiv:1609.05265*, 2016.
- [28] M. Watter, J. Springenberg, J. Boedecker, and M. Riedmiller, "Embed to control: A locally linear latent dynamics model for control from raw images," in *Proc. of Advances in neural information processing systems*, 2015, pp. 2746–2754.
- [29] F. L. Lewis, D. Vrabie, and V. L. Syrmos, *Optimal control*. John Wiley & Sons, 2012.
- [30] D. Vrabie, O. Pastravanu, M. Abu-Khalaf, and F. L. Lewis, "Adaptive optimal control for continuous-time linear systems based on policy iteration," *Automatica*, vol. 45, no. 2, pp. 477–484, 2009.
- [31] D. Kleinman, "On an iterative technique for riccati equation computations," *IEEE Transactions on Automatic Control*, vol. 13, no. 1, pp. 114–115, 1968.
- [32] M. Holmes, A. Gray, and C. Isbell, "Fast svd for large-scale matrices," in *Proc. of Workshop on Efficient Machine Learning at NIPS*, vol. 58, 2007, pp. 249–252.
- [33] A. C. Antoulas, *Approximation of large-scale dynamical systems*. Siam, 2005.
- [34] R. E. Kalman, "Canonical structure of linear dynamical systems," *Proc. of the National Academy of Sciences*, vol. 48, no. 4, pp. 596–600, 1962.
- [35] S. Lall, J. E. Marsden, and S. Glavaški, "Empirical model reduction of controlled nonlinear systems," in *Proc. of IFAC World Congress*, vol. 32, no. 2, 1999, pp. 2598–2603.
- [36] N. Lee and A. Cichocki, "Very large-scale singular value decomposition using tensor train networks," *arXiv preprint arXiv:1410.6895*, 2014.
- [37] T. Ishizaki, K. Kashima, J. Imura, and K. Aihara, "Model reduction and clusterization of large-scale bidirectional networks," *IEEE Transactions on Automatic Control*, vol. 59, no. 1, pp. 48–63, 2013.
- [38] T. Ishizaki, K. Kashima, A. Girard, J. Imura, L. Chen, and K. Aihara, "Clustered model reduction of positive directed networks," *Automatica*, vol. 59, pp. 238–247, 2015.
- [39] M. Mesbahi and M. Egerstedt, *Graph theoretic methods in multiagent networks*. Princeton University Press, 2010.
- [40] R. Albert and A. L. Barabási, "Statistical mechanics of complex networks," *Reviews of modern physics*, vol. 74, no. 1, pp. 47–97, 2002.
- [41] B. Pal and B. Chaudhuri, *Robust control in power systems*. Springer Science & Business Media, 2006.
- [42] T. Sadamoto, A. Chakraborty, T. Ishizaki, and J. Imura, "Dynamic modeling, stability, and control of power systems with distributed energy," *IEEE Control System Magazine*, vol. 39, no. 2, pp. 34–65, 2019.
- [43] A. K. Singh and B. C. Pal, "Decentralized dynamic state estimation in power systems using unscented transformation," *IEEE Transactions on Power Systems*, vol. 29, no. 2, pp. 794–804, 2014.
- [44] K. Kashima, "Noise response data reveal novel controllability gramian for nonlinear network dynamics," *Scientific reports*, vol. 6, no. 27300, pp. 1–8, 2016.